THE 1992 OUTBURST OF THE SU URSAE MAJORIS-TYPE DWARF NOVA HV VIRGINIS1

ELIA M. LEIBOWITZ AND HAIM MENDELSON

Wise Observatory, Sackler Faculty of Exact Sciences, Tel Aviv University, Tel Aviv 69978, Israel

ALBERT BRUCH, HILMAR W. DUERBECK, AND WALTRAUT C. SEITTER

Astronomisches Institut der Universität Münster, Wilhelm-Klemm-Strasse 10, D-48149 Münster, Germany

AND

GEROLD A. RICHTER

Sternwarte Sonneberg, Sternwartestrasse 32, D-96515 Sonneberg, Germany Received 1992 October 21; accepted 1993 August 12

ABSTRACT

The results of 14 nights of photometric monitoring the cataclysmic variable HV Vir, following its outburst in 1992 April, are presented. The star displays all major features of the superhump phenomenon which characterizes the SU UMa class of dwarf novae. A fairly chaotic "early superhump variability" was observed on days 2 and 3 after maximum light, although the occurrence of a superhump structure with a period of $85^{\rm m}$ is already indicated on day 2. The mature superhump structure appeared on day 3.5 and persisted for ~ 20 days, i.e., during the major outburst phases. Its initial period of $84^{\rm m}48^{\rm s}$ decreased in the course of the outburst by 45 s. A stable periodicity of $83^{\rm m}30^{\rm s}.7$, which we interpret as the orbital period, characterizes the photometric behavior of the star during final decline from $\sim 2^{\rm m}$ to $\sim 1^{\rm m}$ above minimum. The superhump shows marked amplitude variations which are related to the difference between superhump and orbital phase. Additional outbursts of HV Vir took place in 1929, 1939, 1970, and 1981. We underline the similarities and differences between HV Vir and two other extreme members of the SU UMa group, compare the photometric behavior of HV Vir with published numerical simulations of the superhump phenomenon, and discuss observable features which might help to establish refined models of the superhump phenomenon.

Subject headings: novae, cataclysmic variables — stars: individual (H Virginis)

1. INTRODUCTION

HV Vir was discovered by Schneller (1931) who found it bright on two sky patrol plates of 1929 February 1 (11^m) and 3 (12^m.5). The reality of the object was confirmed by Duerbeck (1984), who recovered additional images of the 1929 outburst on Harvard plates. On the basis of this evidence, the object received the variable star designation HV Vir and, because of its large amplitude of $\sim 8^{m}$, the classification "nova, not confirmed by spectroscopic observations" (Duerbeck 1987). A second outburst was discovered by Schmeer (1992) on 1992 April 20.9, and follow-up spectroscopic observations showed it to be a dwarf nova on account of its broad absorption lines (Della Valle, Duerbeck, & Motch 1992). Its large amplitude and rare outbursts link it to WZ Sge and related systems.

WZ Sge stars are a hypothetical subclass of the SU UMa type dwarf novae (= UGSU) (Patterson et al. 1981; O'Donoghue et al. 1991). UGSU stars have "superoutbursts," which are longer and brighter than normal outbursts. Regular light variations during superoutbursts are referred to as superhumps (Vogt 1974; Warner 1975), a phenomenon which is the defining characteristic for UGSU stars. The superhump periods are up to a few percent longer than the orbital periods of the systems. WZ Sge stars differ from other UGSU stars by the fact that normal outbursts are rare or apparently lacking and that their superoutbursts have longer durations (several weeks) and larger amplitudes (6^m...9^m). Their orbital periods

are the shortest ones observed for UGSU systems. With only a few well-observed objects, statistics is, however, rather poor.

The origin of the superhump phenomenon is not yet clearly established. The causes presently discussed have largely evolved from the work of Whitehurst (1988) and Osaki (1989), who assume viscous disk instability in systems with small mass ratios with or without enhanced mass transfer from the secondary (Whitehurst & King 1991; Hirose & Osaki 1990, respectively).

Monitoring the photometric behavior of HV Vir during the recent outburst promised to yield information on the nature of WZ Sge stars, as well as an insight into the superhump phenomenon. This was our motivation for initiating a photometric program whose results are presented here.

2. OBSERVATIONS

2.1. Earlier Observations

Observations at minimum light, obtained within ~ 26 months before the current outburst are available, because HV Vir is one of the targets of photometric surveys of novae and related stars at minimum. Howell et al. (1992) found in 1989 March/April V=19.10, B-V=+0.26, V-R=-0.07, and V-J=+1.9. Our CCD observations of 1989 January 11.3 with the Danish 1.5 m telescope at ESO La Silla yield V=19.04, B-V=+0.10 and V-R=+0.14. The maximum magnitude observed around 1992 April 21.4 (Kilmartin 1992), is V=11.5, so that the amplitude of HV Vir is $\Delta V=7.6$.

The Sonneberg plate archive was examined for additional outbursts of HV Vir, and more than 1500 plates, taken between 1928 and 1992, were inspected. Three additional outbursts were found in 1939, 1970, and 1981 (Table 1). The obser-

¹ Based on observations collected at the Wise Observatory, Tel Aviv University, Israel, the European Southern Observatory, La Silla, Chile, and the Sternwarte Sonneberg, Germany.

TABLE 1
PREVIOUS OUTBURSTS OF HV VIR FOUND ON PLATES
OF THE SONNEBERG ARCHIVE

Year	Date	J.D.	$m_{ m pg}$
1939	May 14	2,429,398.48	13.5:
	May 15	399.45	13.5:
	May 16	400.50	13.5:
1970	Feb 1	2,440,619.57	Γ13.5
	Feb 6	624.57	11.2
	Feb 6	624.58	11.6
	Feb 6	624.62	11.3
1981	Mar 27	2,444,691.44	14.2:
	Mar 27	691.47	13.9
	Mar 29	693.42	14.0:
	Mar 30	694.44	[14

vations are not sufficiently detailed to discriminate between superoutbursts and normal outbursts, but the long and probably regular time intervals suggest that they are superoutbursts with a recurrence time of ~ 10 years. There is, however, a caveat since all outbursts were observed in the months February to May, which are the only ones sufficiently well covered by patrol plates. Thus, it is possible that some maxima have gone unnoticed. Using the statistical method of Wenzel & Richter (1986) to determine a "realistic cycle time," 5 or 3 year periods are equally possible.

2.2. Present Observations

Table 2 presents the journal of our observations. Unfiltered high speed photometry was carried out in the first two nights with the 1 m telescope at ESO La Silla and a single channel photometer. The time resolution is 6 s. After every 200 integrations, the sequence was interrupted by measurements of the sky background and a nearby reference star for atmospheric extinction correction. The stability of the reference star suggests an accuracy better than 0\mathbb{m}02 for a single integration. A few additional UBV measurements of HV Vir were also made (Bruch 1992).

All other data were obtained with the RCA CCD camera,

attached to the 1 m telescope of the Wise Observatory in Mitzpe Ramon, through a standard R filter. Until May 19, the integration time was 6 minutes, from May 20 onward 9 minutes. The magnitudes of HV Vir and several neighboring stars were measured in each camera frame using the DAOPHOT CCD photometry package (Stetson 1987). In some nights, photometric standard stars in the globular cluster M92 (Christian et al. 1985) were observed. They were used to determine the standard R magnitudes of the reference stars in the field of HV Vir and, by differential photometry, the R magnitudes of HV Vir. From the light curves of each night the best-fitting gradient and the mean magnitude were subtracted in order to clean the data from long-term brightness variations (timescales of several hours to days).

3. DATA ANALYSIS

3.1. Outburst Light Curve

Figure 1 shows the light curve of HV Vir during the first 50 days following the discovery of the new outburst. Open squares are visual magnitudes reported in IAU Circulars 5502, 5503, 5504, 5516, as well as by Bateson (1992). Filled squares are photoelectric V magnitudes from the Circulars and Bruch (1992). Filled triangles are nightly averages of the R magnitudes from the Wise Observatory. V and R magnitudes are combined into a single light curve, because they are quite comparable during outbursts of dwarf novae below the period gap, to which HV Vir belongs (see § 3.2.1), and for which a mean value $V - R = 0.07 \pm 0.04$ is calculated from the catalog of Echevarría (1984).

The outburst light curve of HV Vir is very similar to that of the 1946 superoutburst of WZ Sge, as displayed in Figure 1 of Patterson et al. (1981), and both systems have the same amplitude of ~7.5. The light curves of both stars show a sharp drop of ~1 within 5 days after maximum, and a rapid decline through 3 between days 25 and 35. This type of brightness evolution appears to be typical for WZ Sge systems, since it is also found in the superoutbursts of several other established or suspected members of the group: VY Aqr, WX Cet, AL Com, V592 Her, and SW UMa (Robinson et al. 1987; O'Donoghue et al. 1991; Richter 1992).

TABLE 2

Log of Observations of HV Vir Following its Outburst in 1992 April^a

D ате (1992)	OBSERVING RUN		INTEGRATION		1.6 D
	(UT)	(JD 2,448,000+)	TIME (minutes)	FILTER	Mean <i>R-</i> Magnitude
Apr 23	3.4-7.1	735.642–735.796	0.1	None	12.12 ^b
Apr 24	3.0-6.8	736.625-736.783	0.1	None	12.45 ^b
Apr 28	18.5-25.3	741.275-741.558	6	R	13.15
May 8	17.9-19.6	751.245-751.320	6	R	14.07
May 9	17.4-24.9	752.231-752.542	6	R	14.15
May 14	20.7-22.3	757.368757.435	6	R	14.36
May 19	19.0	762.292	6	R	17.0
May 20	18.0-20.0	763.253-763.336	9	R	17.03
May 31	17.8-18.2	774.244-774.262	9	R	17.63
Jun 1	18.0-22.4	775.255-775.438	9	R	17.67
Jun 2	18.2-19.6	776.260-776.319	9	R	17.74
Jun 3	18.4-20.1	777.270-777.341	9	R	17.77
Jun 6	17.9-19.5	780.248-780.315	9	R	17.89
Jun 7	18.1-19.6	781.256-781.318	9	R	17.84

^a The first two runs were performed photoelectrically at ESO in La Silla, Chile. All the other observations were performed with a CCD camera at the Wise Observatory in Israel.

b V magnitudes from Bruch 1992.

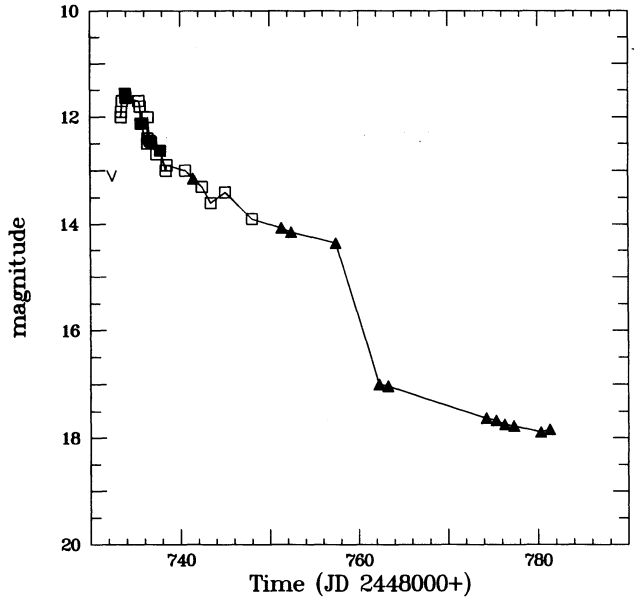


Fig. 1.—The 1992 outburst light curve of HV Vir. Open squares are visual magnitudes as reported in the IAU and the VSS/RASNZ Circulars. Filled symbols indicate photoelectric or CCD measurements. Squares are V magnitudes, and triangles are R magnitudes. V-R is small.

We shall refer to the system prior to its rapid decline, i.e., from 1992 April 20 to May 15, as being in a high state. From May 20 onward, the system will be referred to as being in a low state.

3.2. Periodic Light Variations in HV Vir

Soon after outburst, periodic light variations of HV Vir were reported. Mantel et al. (1992) found a period of either 80 $^{\rm m}$ 6 or 83 $^{\rm m}$ 3 in their observations of April 24/25 and 26/27. A thorough discussion of their observations is given by Barwig, Mantel, & Ritter (1992). Preliminary analysis of our own data of April 28/29 yielded a period 86.1 \pm 2.2 min (Mendelson et al. 1992). Between April 30 and May 1.5, Ingram & Szkody (1992) found superhumps with the period 84 $^{\rm m}$ 1 \pm 0 $^{\rm m}$ 4.

The light curves have amplitudes between 0.06 and 0.25. Often two distinct maxima, the superhump and a secondary hump, are seen, e.g., in the runs of April 28/29 and May 9-10 shown in Figure 2. The presence of the secondary hump was already noted by Barwig et al. (1992) in their observations of April 24/25 and 26/27; it was also seen on April 30 by Ingram & Szkody, while it was absent in their observations of the following night. It was visible again on May 8/9 and 9/10, but is difficult to trace in the observations of May 13/14 (by Roth, Soffner, & Mitsch 1993) and May 14/15.

3.2.1. High State Periodicity

Period search in data sets, which are not much longer than the period itself and separated by long and unequally spaced gaps, is complicated by aliasing. We used power spectra and the analysis of variance (AoV) algorithm (Schwarzenberg-Czerny 1989) and checked the results against each other. After removing the influence of the window function by the CLEAN algorithm (Roberts, Léhar, & Dreher 1987) the almost pure power spectrum of the signal was available. Periodograms calculated with the AoV algorithm provided statistical quality parameters for the data folded with trial periods, while the

aliasing problem remained. Comparisons of the results from both techniques gave a kind of external error.

Periodic variations are clearly visible in the two longest data sets obtained during the high state, taken on April 28/29 and May 9/10. The periodograms of the two nights show the presence of periods in the range 82-86 minutes. The AoV method yielded a pronounced peak for the most probable period of the early observations. The peak decreased, however, when increasingly more data from the later outburst stages were included. We were thus led to the fact that the superhump period P_s is not stable, and subsequently combined only data sets collected during a span of no more than three subsequent nights. To widen our database, we also included the data obtained by Ingram & Szkody (1992) and Roth et al. (1993). The resulting superhump periods are as follows. April 28-May 1: $P_s = 0.05859$; May 8–9: $P_s = 0.05854$; May 13–14: $P_s = 0.05854$ 0.05811. When Barwig et al.'s second period 0.05877, derived for April 25-27, is also included, a smoothly decreasing superhump period is indicated. The zero epoch of the superhump cycle is taken to be HJD 2,448,741.2807, the time of the first superhump observed by the present authors.

The best linear ephemeris for the superhump cycle

$$HJD(max) = 2,448,741.2807 + 0.058645E, \qquad (1)$$

when compared with the observed times of the superhump, yields systematic deviations with an average value of 0.0080 days. This is seen in the corresponding O-C diagram, shown in Figure 3. With the quadratic ephemeris

$$HJD(max) = 2,448,741.2841 + 0.058790E - 7.6 \times 10^{-7}E^2,$$
(2)

the deviations are reduced to an average of 0.0043, and their distribution is almost random. The parabola in Figure 3 represents the quadratic ephemeris.

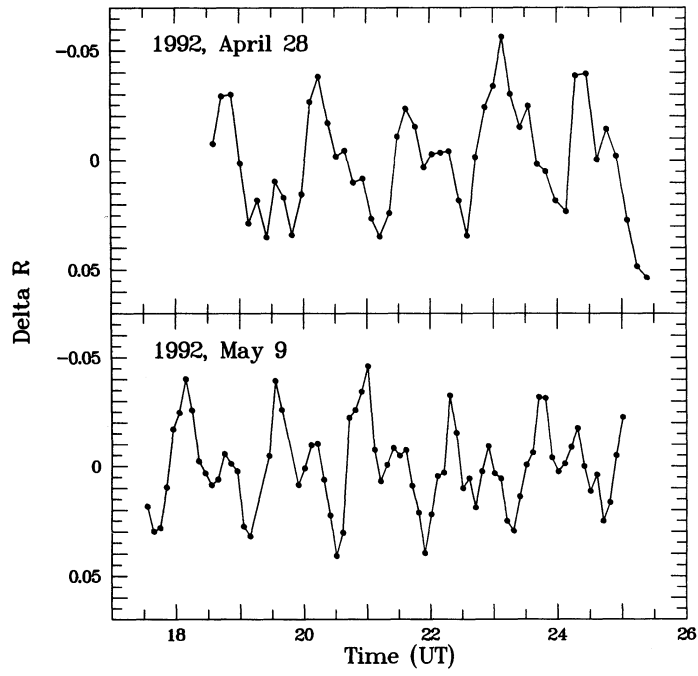


Fig. 2.—R-band light curves of the high state of HV Vir on 1992 April 28/29 (top) and May 9/10 (bottom). Mean values and linear trends have been subtracted.

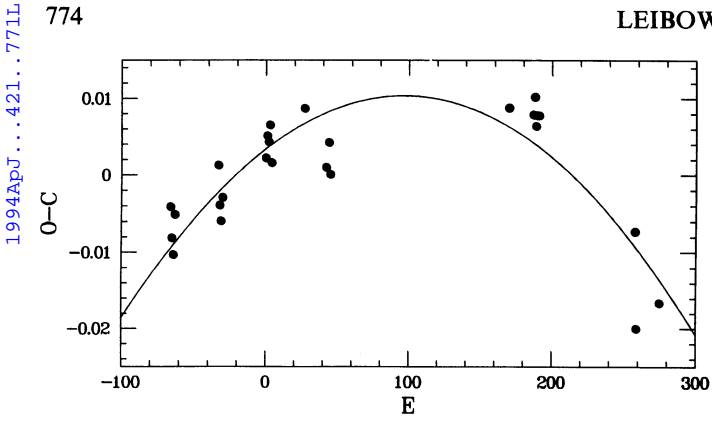


Fig. 3.—0-C diagram of the times of maximum, based on a constant period P = 0.058645. The second-order polynomial, fitted to the O - C values, is shown.

The times of maximum light and the O-C values based on the ephemerides (1) and (2) are given in Table 3. If we assume constant change for the superhump period ($\ddot{P}_s = 0$), we find P_s of 0.05889 at the time of Barwig et al.'s first observations, and $0^{\circ}.05836$ near the end of the high state. The period change is $P_s = (-2.6 \pm 0.2) \times 10^{-5}$. The mean superhump period during the time of observations was $\bar{P}_s = 0.05865 = 84.46$.

The final test for the validity of the ephemeris is the quality of the resulting light curve. Figure 4 includes all available data of the high state, plotted according to ephemeris (2). Different symbols are used for measurements made on different nights. The magnitude variations are significant and will be discussed in § 4.2.1.

So far, the derivation of the light elements was based on O-C data. In the following, the light variations themselves will be used for the determination of P_s and \dot{P}_s . The amplitude

TABLE 3 O-C VALUES OF SUPERHUMP MAXIMA, AS DERIVED FROM THE LINEAR EPHEMERIS (1) AND THE QUADRATIC EPHEMERIS (2)

J.D.hel.(max) (2448000+)	Cycle Number	$ (O-C)_1 $ (days)	$(O-C)_2$ (days)	Observera
737.4060	-66	-0.0041	+0.0053	В
737.4607	-65	-0.0081	+0.0011	В
737.5171	-64	-0.0103	-0.0013	В
737.5810	-63	-0.0051	+0.0037	В
739.3467	-33	+0.0013	+0.0035	В
739.4002	-32	-0.0039	-0.0019	В
739.4568	-31	-0.0059	-0.0041	В
739.5185	-30	-0.0029	-0.0012	В
741.2829	0	+0.0022	-0.0012	W
741.3444	1	+0.0051	+0.0015	W
741.4023	2	+0.0043	+0.0006	W
741.4631	3	+0.0065	+0.0026	W
741.5169	4	+0.0016	-0.0023	W
742.8728	27	+0.0087	+0.0019	I
743.7448	42	+0.0010	-0.0072	I
743.8653	44	+0.0042	-0.0041	I
743.9198	45	+0.0001	-0.0083	I
751.2592	170	+0.0088	+0.0026	W
752.2552	187	+0.0079	+0.0037	W
752.3162	188	+0.0102	+0.0062	W
752.3710	189	+0.0064	+0.0025	W
752.4311	190	+0.0078	+0.0041	W
752.4897	191	+0.0078	+0.0042	W
756.4038	258	-0.0073	+0.0021	R
756.4491	259	-0.0200	-0.0110	R
757.3915	275	-0.0166	-0.0028	w
				• • • • • • • • • • • • • • • • • • • •

^a B, Barwig et al. 1992; I, Ingram & Szkody 1992; R, Roth et al. 1992; W, this paper.

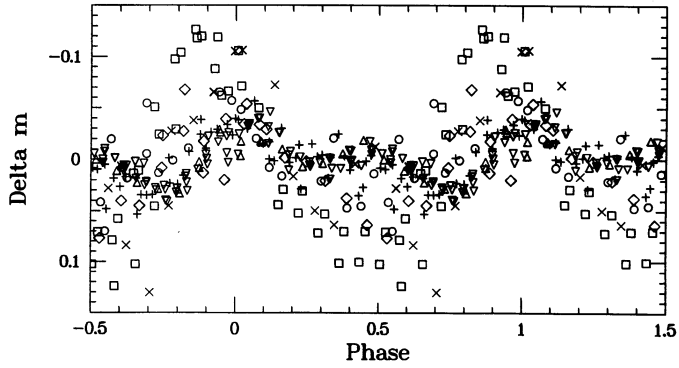


Fig. 4.—Composite R-band light curve of the high state of HV Vir, based on ephemeris (2). Different symbols have been used to identify observations from different nights: pluses (+) for JD 2448741 (April 28/29), crosses (×) for 742 (April 30), open squares (\square) for 743 (May 1), open triangle (\triangle) for 751 (May 8/9), open inverted triangles (∇) for 752 (May 9/10), open diamonds (\diamondsuit) for 756 (May 13/14) and open circles (○) for 757 (May 14/15). Note the large amplitude, the missing secondary hump, and the shift toward earlier phases on JD

of the superhump in HV Vir varies considerably from night to night, complicating phase folding techniques and the use of the χ²-hypersurface. We thus removed this additional timedependent free parameter, which carries no information on the period and period changes, by normalizing all magnitudes to the mean superhump amplitude of the night.

Assuming that the light curve of HV Vir varies as a cosine, with variable period and constant time derivative of the period, the normalized magnitude is expressed by

$$m = -\cos 2\pi \phi(t) . \tag{3}$$

The negative sign accounts for the definition of magnitude. A differential phase increment $d\phi$ of a periodic signal is related to a differential increment in time dt by the relation

$$dt = P_s d\phi . (4)$$

The phase difference at the two instants t_1 and t_0 can be expressed as

$$\phi_1 - \phi_0 = \int_{\phi_0}^{\phi_1} d\phi = \int_{t_0}^{t_1} \frac{dt}{P_s}.$$
 (5)

Assuming the period to have a constant time derivative

$$\phi_1 - \phi_0 = \frac{1}{\dot{P}_s} \ln \left(\frac{P_{t_1}}{P_{t_0}} \right), \tag{6}$$

where P_{t_0} and P_{t_1} are the superhump periods at the times t_0 and t_1 , respectively. $\chi^2(P_s, \dot{P}_s, t_0)$ is given by

$$\chi^2 = \sum_{i=1}^n (m_i + \cos 2\pi \phi_i)^2.$$
 (7)

To reduce the number of free variables, the time t_0 is taken from the observations and is allowed to vary only slightly to account for observational uncertainties.

The parameter combinations yielding χ^2 -minima are determined with the simplex algorithm (Nelder & Mead 1965). The results depend strongly on the initial values and their initial increments. The χ^2 -hypersurface shows deep minima for

Solution 1:
$$P_s = 0.05843$$
, $\dot{P}_s = -0.0000126$;

Solution 2:
$$P_s = 0.05879$$
, $\dot{P}_s = -0.0000257$;

Solution 3:
$$P_s = 0.05895$$
, $\dot{P}_s = -0.0000445$.

No. 2, 1994

3.2.2. Early High-State Periodicity and High-Frequency Oscillations

The light curves of April 23 and 24 (Fig. 5) will be referred to as early high-state light curves. The maxima predicted by ephemeris (2) are clearly seen on April 23. On April 24, the light curve appears more chaotic and rather flat, showing no oscillation with a period near 85 minutes. As will be shown in § 4.2.1, the superhump amplitudes are modulated by the phase shift between the superhump period and the orbital period. According to this, the superhumps occurred with almost maximum amplitude on April 23, while on April 24, they are expected to be lower by a factor 2. Since in the measured early superhump the maximum amplitude is lower by a factor of 2-3, compared to that of the mature superhump, we postulate that the superhump amplitudes during early outburst are generally lower by this factor. This explains why the superhumps near the amplitude minimum, which occurred on April 24, are lost in the flickering.

The high-speed photometry of April 23 and 24 allows us to investigate the presence or absence of coherent light variations, down to periods of a few seconds. The light curve shows that the brightness of the system varied during these two nights on timescales from hours to the Nyquist period of 12 s. Fourier analysis of the two light curves, however, did not reveal significant coherent oscillations. Tests, consisting of adding artificial sinusoidal signals to the light curve, show that coherent variations with amplitudes as small as 0\(^m\).002 could have been easily detected. This result is in good agreement with the findings of Patterson et al. (1993) for VY Aqr.

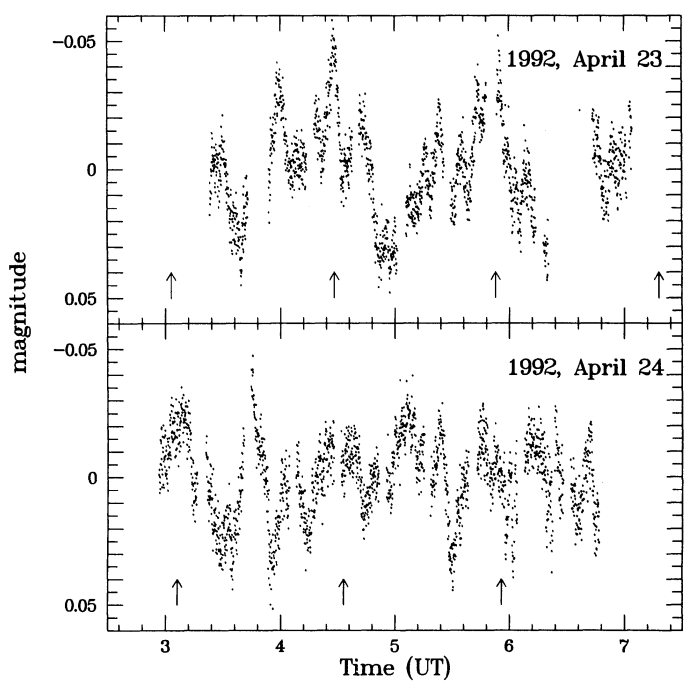


Fig. 5.—White-light high-speed light curves of the early high state of HV Vir on 1992 April 23 and 24. Mean values and linear trends have been subtracted. The expected times of superhump maxima are indicated by arrows.

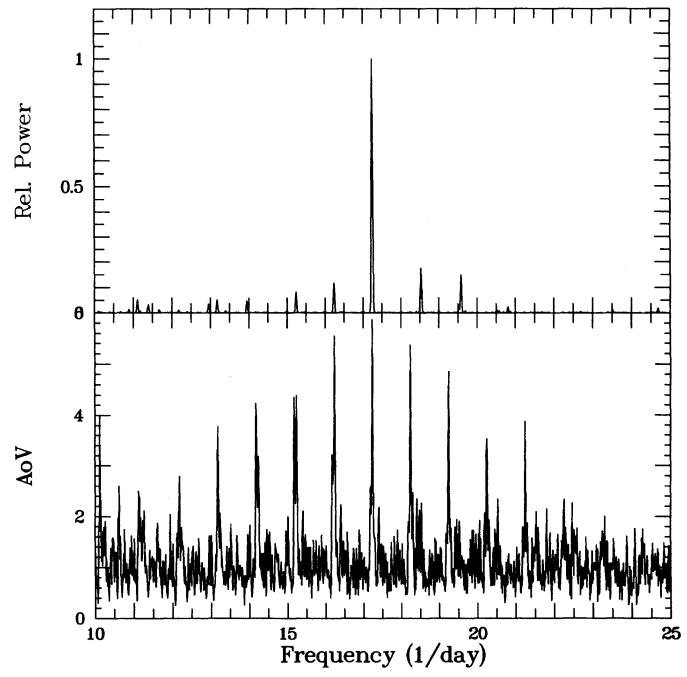


FIG. 6.—Cleaned power spectrum (top) and AoV diagram (bottom) of the low-state observations of HV Vir. In both diagrams, the highest peak indicates orbital period.

3.2.3. Low-State Periodicity

Most observing runs in the low state of HV Vir (with the exception of the measurements of June 1) lasted for 2 hr or less. Nevertheless, there is a cyclic variation in the brightness of the star apparent in each of these runs, showing an amplitude of $\sim 0^{m}$ 2 and a period of $\sim 83^{m}$.

The power spectrum of all our low state data yields a period of $0^{\circ}.057995 \pm 0^{\circ}.000047$, where the error is calculated from the resolution of the power spectrum. From AoV analysis, we obtain the period $0^{\circ}.057994 \pm 0^{\circ}.000048$, with the error derived from the one half-width of the corresponding peak in the periodogram. For the final low state period, which we identify with the orbital period P_0 , we adopt the mean from the two methods $P_0 = 0^{\circ}.05799 \pm 0^{\circ}.00003 = 83^{\circ}.512 \pm 0^{\circ}.043$. The cleaned power spectrum and the AoV periodogram are shown in Figure 6. Figure 7 shows the low-state data folded on P_0 ,

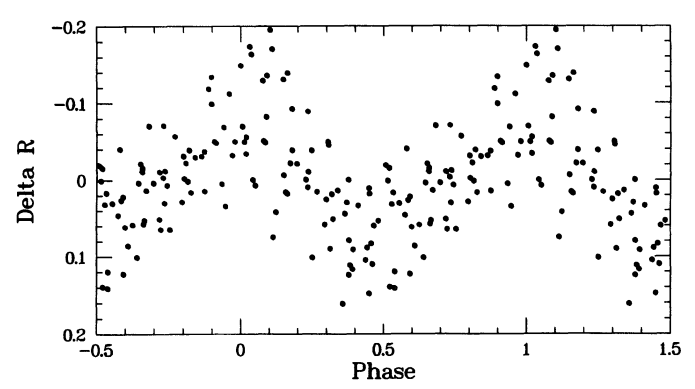


Fig. 7.—Low-state light curve of HV Vir, folded on the orbital period P_0

776

according to the ephemeris of maximum light in the low-state:

$$HJD(max) = 2,448,763.2739 + 0.05799E \tag{9}$$

4. DISCUSSION

4.1. Periodicities

Since superoutbursts of SU UMa systems are characterized by superhumps, their presence in HV Vir confirms its membership in this class of dwarf novae. The light curves in Figure 2 show that quite often the superhump is followed by a secondary hump, and that the superhump structure is spread over the entire period, as in VW Hyi (Schoembs & Vogt 1980; Duerbeck & Vogt 1984; van Amerongen, Bovenschen, & van Paradijs 1987) and WZ Sge (Patterson et al. 1981) and not restricted to a confined phase range as in Z Cha (Kuulkers, van Amerongen, & van Paradijs 1991), OY Car (Schoembs 1986; Naylor et al. 1987) and TU Men (Stolz & Schoembs 1984).

4.1.1. Evolution of the Superhump Period

On April 24.8 the mature superhump was visible and lasted until the sudden decline from the high state on May 15. Already on April 23.2, 2 days after the outburst maximum, superhump maxima of lower amplitude were observed at the times predicted by ephemeris (2). O'Donoghue et al. have suggested that in short-period SU UMa systems, the superhump appears ~1 week after outburst. The early onset in HV Vir shows that there is at least one exception. It would be interesting to search the other short-period systems for early low amplitude superhumps, which might have eluded detection.

The O-C diagram for all observed primary superhump maxima (Fig. 3) indicates a decrease of the superhump period, as is found in all well-investigated SU UMa systems (Patterson et al. 1993). During the 21 days of superhump visibility, the superhump period decreased with $\dot{P}_s = -2.6 \times 10^{-5}$. HV Vir has the smallest change observed so far, which strengthens the case for the tendency of short period (= low-mass ratio) systems showing smaller period changes. The few exceptions, where the period appears to increase (e.g., OY Car; Krzeminski & Vogt 1985) certainly warrant closer study.

4.1.2. Period Excess

The period excess observed in HV Vir must be confirmed by measurements of the orbital period P_0 during minimum. We are, however, quite confident to have found the minimum period already in our observations taken after the rapid decline, when the star was between 2 and 1 mags above minimum. In VW Hyi, the orbital period also appeared between 2 and 1 mag above minimum (Haefner, Schoembs, & Vogt 1979).

With the above value, the fractional period excess in HV Vir

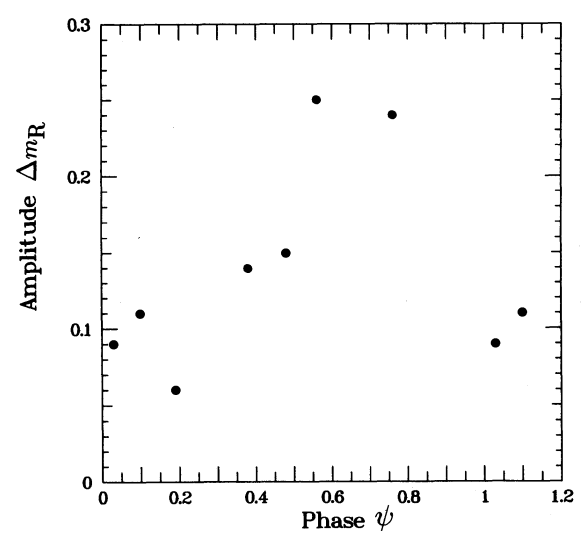


Fig. 8.—The amplitude of the superhump light variation Δm_R is shown as a function of the lag ψ of the orbital phase with respect to the superhump variability.

is $(\bar{P}_s - P_0)/P_0 = \Delta P/P_0 = 0.0114$ or 1.14%. This is comparable to the value 0.8% of WZ Sge while all other SU UMa systems have period excesses of several percent (disregarding the uncertain period excess of BR Lup; see Table 1 in Molnar and Kobulnicky 1992).

4.2. Photometric features

4.2.1. Variation of Superhump Amplitude

Table 4 gives the observed superhump amplitudes ($\Delta m_R = m_{\rm max} - m_{\rm min}$) for the individual nights, and the corresponding times of maximum light $t_{\rm max}$ for both the superhump and the orbital period. In nights where several cycles were observed, these times refer to the first cycle only, since changes in phase difference between the superhump and orbital maxima are negligible with a given night. The folded light curve of the high state (Fig. 4) shows large variations in the amplitudes, notably on April 30 and May 1 (JD 2,448,742–743), which suggest a systematic effect.

With the phases ψ of orbital maximum light in the superhump cycle for each night given by

$$\psi = \frac{t_{\text{max}}(\text{orbit}) - t_{\text{max}}(\text{superhump})}{\bar{P}_{s}},$$
 (10)

and also listed in Table 4, it became apparent that the amplitude of the superhump light variation depends on ψ as shown in Figure 8. The largest amplitudes occur when orbital phase 0

TABLE 4 Phase Shift ψ between Times of Maximum Light $t_{\rm max}$ for the Superhump and Orbital Periods, and Amplitude of Light Variation in the High State

Day (1992)	Cycle Number	t_{max} (superhump) J.D.	t _{max} (orbit) J.D.	ψ (phase)	Amplitude Δm_R
Apr 28/29	2	741.4017	741.4079	0.11	0.11
Apr 30	27	742.8709	742.9159	0.77	0.24
May 01	43	743.8107	743.8439	0.57	0.25
May 8/9	170	751.2564	751.2679	0.20	0.06
May 9/10	188	752.3098	752.3119	0.04	0.09
May 13/14	258	756.4013	756.4299	0.40	0.15
May 14/15	275	757.3939	757.4159	0.38	0.14

coincides with superhump phase 0.65, smallest amplitudes occur when orbital phase 0 coincides with superhump phase 0.15. The period of the amplitude variation is the beat period between superhump and orbital period.

According to current models (Hirose & Osaki 1990), the superhump is caused by enhanced dissipation in an eccentric accretion disk and occurs preferentially during a certain phase interval of the superhump period. The disk luminosity during superoutburst is thus variable with the superhump period. It may also depend on the aspect of the disk presented to the observer. For a fixed phase of the superhump period, e.g., maximum light, the aspect varies with the beat between superhump and orbital period. Thus the amplitude of the superhump, as seen by the observer, also varies with the beat period, as is observed in HV Vir.

This effect may be enhanced by the reflection of maximum light off the secondary which would also be modulated with the same period. Alternatively, the superhump light source itself might have a variable amplitude as is indicated by Hirose & Osaki (their Fig. 8), although this figure does not permit to decide whether the superhump variation in the simulations is monotonic or modulated with the beat period.

4.2.2. Decrease of Superhump Periods and Brightness Decline in SU UMa outbursts

Patterson et al. (1993) have drawn attention to a correlation between the change of the superhump period and the brightness decline in SU UMa outbursts. From our four high-state magnitudes in the R band and the actual periods from ephemeris (2), we obtain

$$dP_s/dm_R = -0.45 \pm 0.06 \text{ mag}^{-1}. \tag{11}$$

Since the rate of decline is expected to be proportional to the period P_s , the value of $(1/P_s)dP_s/dm$ should be the same for all systems. For HV Vir we derive

$$(1/P_s)dP_s/dm_R = -0.0053 \pm 0.0007 \text{ mag}^{-1}$$
, (12)

as compared to the mean relation in the V-band for eight other systems

$$(1/P_s)dP_s/dm_V = -0.0064 \pm 0.0010 \text{ mag}^{-1}$$
 (13)

by Patterson et al. (1993). Because of the color neutrality during outburst (see § 3.1) our result confirms the validity of their relation. For small variations we can then use the approximation

$$\frac{dP_s}{P_s} \approx 0.006 \, \frac{dL}{L} \,, \tag{14}$$

where L is the luminosity of the system. This relation underlines the tight correlation between the expended outburst energy and the evolution of the accretion disk.

4.3. Mass Ratio of the System

The fractional period excess of the (average) superhump period is expected to depend on the mass ratio of the binary components (Whitehurst & King 1991). Figure 2 of Molnar & Kobulnicky (1992) provides observational evidence for such a relation, and permits the empirical estimate of the mass ratio of HV Vir from the superhump period. A linear relation between mass ratio and period excess yields

$$q = m_2/m_1 = 0.14 \pm 0.07 \ . \tag{15}$$

Next to mass ratio in GD 552 (Hessman & Hopp 1990), this appears to be the most extreme mass ratio of dwarf novae

observed so far. It makes HV Vir an interesting target for spectroscopic observations.

5. IMPLICATIONS CONCERNING THE ORIGIN OF THE SUPERHUMP PHENOMENON

5.1. Structural Evidence

Observations presented here support models in which the structure of the superhump depends on the (somewhat variable) mass distribution in the accretion disk of the cataclysmic binary; modulated light variations, as shown in Figure 8, give information on the location of the major mass concentration in the disk. Detailed numerical simulations of the light output over a complete beat cycle between the orbital and the superhump period should provide a test for this empirical finding.

The role of superoutbursts in the evolution of close binary systems is discussed in the following.

5.2. Evolutionary Evidence

Orbital and superhump periods given by Molnar & Kobulnicky (1992) and the periods of HV Vir presented in this paper improve the empirical relation of period excess versus orbital period detected by Stolz & Schoembs (1981) and updated by Robinson et al. (1987). Figure 9 shows the linear fit to 13 of 19 known UGSU stars, excepting TU Men because of its long period, T Leo, because its mass ratio is much larger than expected for UGSU stars, and VY Aqr, AW Gem, BR Lub and TY Psc, because of the large uncertainties in their periods. The correlation coefficient is 0.9 for the linear fit to the systems shown in Figure 9.

According to the figure, the difference between P_0 and P_s ceases to exist at periods of $\sim 69^{\rm m}$. The empirical mass ratio for $\Delta P=0$, extrapolated from the systems listed in Molnar & Kobulnicky (1992) is $m_2/m_1\approx 0.12$. For a white dwarf binary of maximum mass this corresponds to a minimum mass of the secondary of $m_2=0.17~M_{\odot}$. For less massive white dwarfs, the

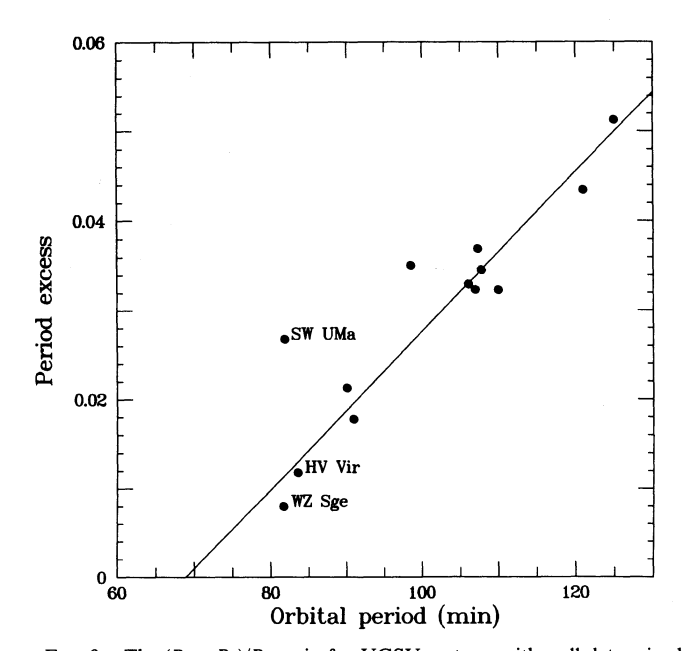


Fig. 9.—The $(P_s-P_0)/P_0$ ratio for UGSU systems with well-determined periods. The best linear fit (omitting the deviating point of SW UMa) is used to determine the hypothetical period P=68.9 minutes, at which the superhump and orbital variations can no longer be distinguished.

 ${\bf TABLE~5}$ Measured Parameters Related to the Superhump Phenomenon in Three SU UMa Systems

Parameter	WZ Sge	SW UMa	HV Vir	
Amplitude of outburst (mag)	8.0	7.0-7.5	7.6	
Recurrence time (yr)	32.5	1.27	3 10.5	
Outburst duration (days)	30	22	28	
Superhump onset time (days after maximum)	10	≈8	2	
Superhump amplitude (%)	≈10	11	6 10	
Orbital period (minutes)	81.629	84.0	84.47	
Period excess (%)	0.8	2.7	1.15	
Superhump period change $(10^5 \ \vec{P})$	1 ± 4	?	2.5 ± 0.2	

Notes:—Additional sources are Patterson et al. 1981 for WZ Sge, and Robinson et al. 1987 for SW UMa.

very low masses of the secondaries would lead to rapid decay of the orbits, followed by the evolution of the nondegenerate objects into degeneracy and an increasing size of the orbit.

These numbers match fairly well with those found in the evolutionary scheme of Paczyński (1981), Rappaport, Joss, & Webbink (1982) and Paczyński & Sienkiewicz (1983), where the theoretical lower stability limit is $P_0 = 57^{\rm m}$ for mainsequence stars of mass $M = 0.085~M_{\odot}$. The fact that nearly the same limits hold for the existence of systems with nondegenerate secondaries and for the occurrence of the superhump phenomenon leads to the conclusion that the UGSU systems, and WZ Sge stars in particular, are associated with very late stages of cataclysmic binary evolution. To a high percentage, the systems belong to the halo systems of Howell & Szkody (1990), and thus are considered to be old.

6. SUMMARY

A summary of major findings of our photometric study of the 1992 outburst of HV Vir is given in Table 5, together with the relevant properties of WZ Sge and SW UMa, two systems with similar orbital periods. WZ Sge has very rare superoutbursts (cycle time 33 years), HV Vir rare superoutbursts (cycle time 3-10 yr), SW UMa frequent superoutbursts (average cycle time 1.25 yr). All of them appear to have no normal outbursts, which might be taken as a classifying criterion for WZ Sge stars until there is evidence to the contrary.

HV Vir is a valuable addition to the sparsely populated group of WZ Sge stars among the UGSU class of dwarf novae. It offers some aspects which may allow refinements of superhump models, especially since the superhump phenomenon in HV Vir was covered from its beginning, 2 days after the superoutburst, to the onset of its rapid decline. Early small amplitude brightness variations with the period of the superhump developed rapidly into mature superhump variations with a 2–3 times larger amplitude. The amplitudes were always modulated by the beat between orbital and superhump period.

Observational details lend further support to the general models of disk evolution during outbursts as suggested by Whitehurst (1989), Hirose & Osaki (1990), and Whitehurst & King (1991). Refined models might be able to explain the close relation between the luminosity evolution in the superoutburst and the dynamical evolution of the disk.

We cordially thank the German-Israeli Foundation for Scientific Research and Development (GIF) for supporting this project, P. Schmeer for immediate information on his discovery of the new outburst of HV Vir, H. Barwig and M. Roth (Universitätssternwarte Munich) as well as P. Szkody (Astronomy Department, University of Washington) for timely preprints that were essential for the disentangling of periodicities.

REFERENCES

Barwig, H., Mantel, K.-H., & Ritter, H. 1992, A&A, 266, L5
Bateson, F. M. 1992, Var. Star Circ. Roy. Astron. Soc. New Zealand, M92/6
Bruch, A. 1992, Inf. Bull. Var. Stars, No. 3745
Christian, C. A., Adams, M., Barnes, J. V., Butcher, H., Hayes, D. S., Mould, J. R., & Siegel, M. 1985, PASP, 97, 363
Della Valle, M., Duerbeck, H. W., & Motch, C. 1992, IAU Circ., No. 5503
Duerbeck, H. W. 1984, Inf. Bull. Var. Stars, No. 2502
——. 1987, Space Sci. Rev., 45, 1
Duerbeck, H. W., & Vogt, N. 1984, Veröff. Astron. Inst. Bonn, No. 97
Echevarria, J. 1984, Rev. Mexicana Astron. Af., 9, 99
Haefner, R., Schoembs, R., & Vogt, N. 1979, A&A, 77, 7
Hessman, F. V., & Hopp, U. 1990, A&A, 228, 387
Hirose, M., & Osaki, Y. 1990, PASJ, 42, 135
Howell, S. B., & Szkody, P. 1900, ApJ, 356, 623
Howell, S. B., Wagner, R. M., Bertram, R., & Szkody, P. 1992, IAU Circ., No. 5505
Ingram, D., & Szkody, P. 1992, Inf. Bull. Var. Stars, 3810
Kilmartin, P. M. 1992, IAU Circ., No. 5503
Krzeminski, W., & Vogt, N. 1985, A&A, 144, 124
Kuulkers, E., van Amerongen, S., & van Paradijs, J. 1991, A&A, 252, 605
Mantel, K. H., Barwig, H., Patschke, M., & Ritter, H. 1992, IAU Circ., No. 5517
Mendelson, H., Leibowitz, E. M., Brosch, N., & Almoznino, E. 1992, IAU Circ. No. 5509
Molnart, L. A., & Kobulnicky, H. A. 1992, ApJ, 392, 678
Naylor, T., Charles, P. A., Hassall, B. J. M., Bath, G. T., Berriman, G., Warner, B., Bailey, J., & Reinsch, K. 1987, MNRAS, 229, 183
Nelder, J. A., & Mead, R. 1965, Comput. J., 7, 308
O'Donoghue, D., Chen, A., Marang, F., Mittaz, J. P. D., Winkler, H., & Warner, B. 1991, MNRAS, 250, 363

Osaki, Y. 1989, PASJ, 41, 1005 Paczyński, B. 1981, Acta Astron., 31, 1 Paczyński, B., & Sienkiewicz, R. 1983, ApJ, 268, 825 Patterson, J., Bond, H. E., Grauer, A. D., Shafter, A. W., & Mattei, J. A. 1993, PASP, 105, 69 Patterson, J., McGraw, J. T., Coleman, L., & Africano, J. L. 1981, ApJ, 248, Rappaport, S., Joss, P. C., & Webbink, R. F. 1982, ApJ, 254, 616 Richter, G. A. 1992, in Reviews in Modern Astronomy, Vol. 5, ed. G. Klare (Berlin: Springer), 26 Roberts, D. H., Léhar, J., & Dreher, J. W. 1987, AJ, 93, 668 Robinson, E. L., Shafter, A. W., Hill, J. A., & Wood, M. A. 1987, ApJ, 313, 772 Roth, M. M., Soffner, T., & Mitsch, W. 1993, in IAU Symp. 155, Planetary Nebulae, ed. R. Weinberger & A. Acker (Dordrecht: Kluwer), 487 Schmeer, P. 1992, IAU Circ., No. 5502 Schneller, H. 1931, Astron. Nachr., 243, 335 Schoembs, R. 1986, A&A, 158, 223 Schoembs, R., & Vogt, N. 1980, A&A, 91, 25 Schwarzenberg-Czerny, A. 1989, MNRAS, 241, 153 Stetson, P. B. 1987, PASP, 99, 191 Stolz, B., & Schoembs, R. 1981, Inf. Bull. Var. Stars, No. 2029 van Amerongen, S., Bovenschen, H., & van Paradijs, J. 1987, MNRAS, 229, Warner, B. 1975, MNRAS, 170, 219 Wenzel, W., & Richter, G. A. 1986, Astron. Nach., 307, 209 Whitehurst, R. 1988, MNRAS, 232, 35

Whitehurst, R., & King, A. R. 1991, MNRAS, 249, 25